CORONARY ARTERY MOTION MODELING FROM 3D CARDIAC CT SEQUENCES USING TEMPLATE MATCHING AND GRAPH SEARCH

Dong Ping Zhang[a*], *Laurent Risser*[a,b], *Coert Metz*[c], *Lisan Neefjes*[d]
Nico Mollet[d], *Wiro Niessen*[c], *Daniel Rueckert*[a]

[a] Department of Computing, Imperial College London, London, UK
[b] Institute for Mathematical Science, Imperial College London, London, UK
[c]Dept. of Medical Informatics and Radiology, Erasmus MC, University Medical Center, Rotterdam, NL
[d]Dept. of Radiology and Cardiology, Erasmus MC, University Medical Center, Rotterdam, NL

ABSTRACT

In this paper we present a method for coronary artery motion tracking in 4D cardiac CT data sets. The algorithm allows the automatic construction of a 4D coronary motion model from pre-operative CT which can be used for guiding totally-endoscopic coronary artery bypass surgery (TECAB). The proposed approach is based on two steps: In the first step, the coronary arteries are extracted in the end-diastolic time frame using a minimal cost path approach. To achieve this, the start and end points of the coronaries are identified interactively and the minimal cost path between the start and end points is computed using the A* graph algorithm. In the second stage the coronaries are tracked automatically through all other phases of the cardiac cycle. This is achieved by automatically identifying the start and end points in subsequent time points through a non-rigid template-tracking algorithm. Once the start and end points have been located, the minimal cost path is constructed in every time frame. We compare the proposed approach to two alternative approaches: The first one is based on a semi-automatic extraction of the coronaries with start and end points manually supplied in each time frame and the second approach is based on propagating the extracted coronaries from the end-diastolic time frame to other time frames using non-rigid registration. Our results show that the proposed approach performs significantly better than non-rigid registration based method and that the resulting motion model is comparable to the motion model constructed from semi-automatic extractions of the coronaries.

***Index Terms*—** Image Registration, Motion Detection and Tracking, Image Guided Surgery, Cardiovascular Image Analysis

1. INTRODUCTION

As one of the leading causes of death worldwide, coronary artery disease occurs due to the failure of blood circulation to supply adequate oxygen and nutrition to cardiac tissues. It is typically caused by the excessive accumulation of atheromatous plaques and fatty deposits within certain regions of the arteries which restricts the blood flow. To treat this disease, arteries or veins grafted from the patient's body are used to bypass the blockages and restore the supply to the heart muscle. Based on image-guided robotic surgical system, totally endoscopic coronary artery bypass (TECAB) surgery has been developed to allow clinicians to perform the bypass surgery off-pump with three pin-hole incisions in the chest cavity, through which two robotic arms and one stereo endoscopic camera are inserted. However, 20-30% conversion rates from TECAB surgery to the conventional invasive surgical approach [1, 2] have been reported due to the vessel misidentification and mis-localization caused by the restricted field of view of the stereo endoscopic images.

The goal of our work is to construct a patient-specific 4D coronary artery motion model from preoperative cardiac CT sequences. By temporally and spatially aligning this model with the intraoperative endoscopic views of the patient's beating heart, we expect to assist the surgeon to identify and locate the correct coronaries during the TECAB procedures [3, 4].

In previous work, Shechter *et al.* [5, 6] tracked coronary artery motion in a temporal sequence of biplane X-ray angiography images. In their approach, a 3D coronary model is reconstructed from extracted 2D centrelines in end-diastolic angiography images. The deformation throughout the cardiac cycle is then recovered by a registration-based motion tracking algorithm. The disadvantage is that 3D reconstruction of the coronary is required. An alternative approach for the extraction of the coronaries from cardiac CT has been proposed by Metz *et al.* [7]: Here the coronaries are manually or semi-automatically identified at one time frame and then tracked throughout the cardiac cycle using non-rigid registration of the multi-phase cardiac CT images. The restriction of this approach is that highly localized motion of the coronaries can not be fully recovered by the motion tracking of the entire heart.

In this paper, we present an approach for coronary motion tracking in cardiac CT images which significantly improves the accuracy of motion tracking and reduces the manual interaction. The proposed approach is based on an template fitting and tracking algorithm which automatically identifies the start and end points of each vessel in every time frame. Once the start and end points have been identified the vessel is extracted as the minimal cost path between both points. The proposed approach is compared to a registration based approach similar to the one presented by Metz *et al.* [7] and to manual tracking of the coronaries. This simplifies the 4D motion modeling of the coronaries significantly.

2. METHOD

We first use contrast limited adaptive histogram equalization to improve the image contrast. Due to the ECG pulsing windows applied in the acquisition and reduced radiation dose [8], the signal-to-noise ration is varying in the multiple-phase 4D data sets. To improve the image quality, anisotropic filtering is used to reduce this noise and preserve the cardiac chamber boundaries and vessel structures.

Using Euclidean distance as the heuristic term, A* graph search is performed at each phase in each dataset to extract the coronaries, based on user-supplied start and end points for each vessel. We then model the coronary motion using the hierarchy non-rigid registration of the CT sequence. Last but most importantly, small vessel template estimation and fitting is proposed to identify the starting and ending points of the coronaries. Combined with graph search, this enables the automatic identification of seed points in each vessels and also utilizes the accurate extraction of vessel paths based on minimal cost graph search approach. We then compare the template based approach with the non-rigid registration one by performing non-parametric Kruskal-Wallis test.

2.1. Image Preprocessing

Before coronary artery extraction, the contrast in the cardiac CT image sequences is enhanced by performing contrast limited adaptive histogram equalization [9]. This improves the visibility of the coronary arteries. Note that this step is carried out for the entire image sequences so that intensities in all time frames are treated similarly. After this contrast enhancement, we perform 4D anisotropic diffusion [10] to smooth the image sequence spatially and temporally while preserving edges and other salient features. Anisotropic diffusion is performed by using a semi-implicit ADI scheme that is shown to be stable and much faster than classical explicit scheme.

2.2. Identification of the coronary artery centerline using minimal cost path

We first perform a coarse segmentation of the coronary arteries in the CT image using a multiscale Hessian-based vessel enhancement filter [11]. The filter utilizes the 2nd-order derivatives of the image intensity after smoothing (using a Gaussian kernel) at multiple scales to identify bright tubular-like structures with various diameters. The six second-order derivatives of the Hessian matrix at each voxel are computed by convolving the image with second-order Gaussian derivatives at a pre-selected scale value.

Assuming a 3D image function $I(\mathbf{x})$, the Hessian matrix at a given voxel $\mathbf{x}$ at scale σ is denoted as $H_\sigma(\mathbf{x})$. A vesselness term $V(\mathbf{x})$ is defined as in Frangi *et al.* [11] and is based on the eigenvalues and eigenvectors of $H_\sigma(\mathbf{x})$. The vesselness response is computed at a series of scales. The maximum response of the vesselness filter at the corresponding optimal scale is obtained for each voxel of the image. Once the vesselness at each voxel is computed it can be used to define a minimal cost path between the start and end nodes. The minimal cost path between the start S and end node E is obtained using the A* graph search algorithm [12] in the end-diastolic CT image. The location of the pair of nodes S and E is specified semi-interactively. The uni-directional graph search algorithm evaluates the smallest cost from node S to current node $\mathbf{x}$ denoted as $g(\mathbf{x})$ and the heuristic cost from current node to node E denoted as $h(\mathbf{x})$ to determine which voxel to be selected as next path node. The search algorithm finds the optimal path only if the heuristic underestimates the cost. The Euclidean distance from $\mathbf{x}$ to E is used to calculate the heuristic cost in our application. We assess each candidate node by calculating the cost $f(\mathbf{x})$ as:

$$f(\mathbf{x}) = g(\mathbf{x}') + \frac{1}{V(\mathbf{x}) + \epsilon} + \delta h(\mathbf{x}). \tag{1}$$

where $g(\mathbf{x}')$ is the score of previous node. To initialize the cost function, $g(\mathbf{x}')$ is set to be zero for the starting node S. ϵ is a small positive constant added in to avoid the singularities. Parameter δ is estimated as the ratio of the minimum cost of the vessel to the Euclidean distance of the starting and ending nodes. By using the heuristic term, the searching space is greatly reduced and the minimum cost path can be found in real-time. When node E is reached, the minimum cost path is reconstructed by tracing backwards to node S. The algorithm finds a minimal cost path consisting of an ordered set of discrete locations (voxels). After extraction of the path we estimate a B-spline representation of the centreline of the coronaries that smoothly interpolates these voxel locations.

2.3. Method 1: Coronary motion tracking using non-rigid image registration

The first approach for tracking the coronaries throughout the cardiac CT sequence is based on non-rigid registration: The coronary motion is obtained by estimating cardiac motion based on non-rigid image registration using a free-form deformation model based on cubic B-splines [13]. A series of registration steps is performed to register each time frame to the reference image at end-diastolic phase. For each frame we use the previous registration results as initial estimation as shown in the middle row of Fig 1. Each registration proceeds in a multi-resolution fashion, starting with a control point spacing of 40mm and ending with a spacing of 5mm. The non-rigid registration algorithm uses normalised mutual information as the similarity measure between time frames. A gradient descent optimization is used to find the optimal transformation. The extracted coronary arteries in the end-diastolic phase are mapped to the other cardiac phases by applying the deformation obtained from the finest registration step as illustrated in the bottom row of Fig 1.

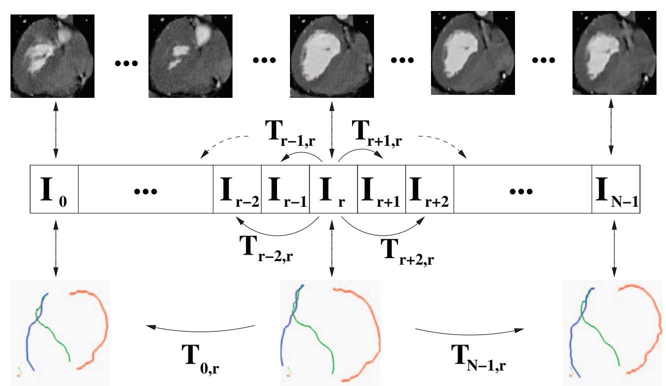

Fig. 1. Illustration of coronary motion tracking using a non-rigid registration approach

2.4. Method 2: Coronary motion tracking using template fitting

The second approach for tracking the coronaries throughout the cardiac CT sequence is based on template localization and fitting. A tubular segment model [14] is adopted to map a spatial coordinate $\mathbf{x}$ to the intensity range $[0, 1]$ through a template function $M(\mathbf{x}; r, \mathbf{x}_0, \vec{v})$. The template function defines an ideal vessel segment centered at point $\mathbf{x}_0$ running in the $\vec{v}$ direction with radius r. A vessel profile is defined to model the image intensity variation in the cross-sectional plane perpendicular to the vessel direction.

Given the coronary centrelines extracted in the end-diastolic time frame as shown in Fig. 2, the start and end points are selected from each vessel centerline as the locations of the centers of the vessel templates. The optimal vessel template together with the

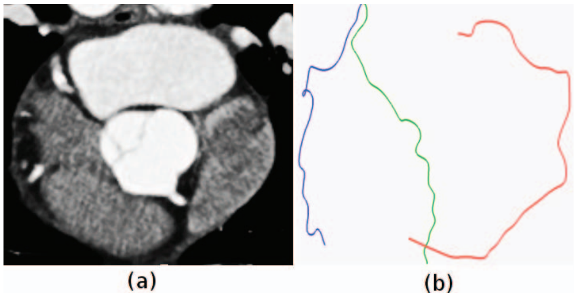

Fig. 2. (a) Post-processed end-diastolic image, (b) its extracted coronary centerlines. Right coronary artery is shown in red, left anterior descending artery in green, left circumflex artery in blue.

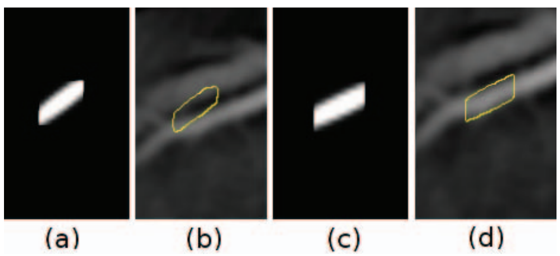

Fig. 3. Illustration of template estimation and fitting. (a) Initial estimation of the template and (b) its mismatch with the vessel segment. The template (a) is shown as yellow contour. (c) Fitted template after optimization and (d) its overlap with the vessel segment.

corresponding local contrast and local mean intensity parameters are obtained by solving the weighted least squared problem using Levenberg-Marquardt algorithm [14] in the end-diastolic time frame. We then transform the center location $\mathbf{x}_0$ of each template to its new estimated position $\mathbf{x}_0'$ in the adjacent time frame by using the deformation information obtained in Section 2.3. The direction and radius estimates for each template at previous phase are used to initialize the corresponding template at current time frame. The template parameters are optimized again using Levenberg-Marquardt optimization. After this the minimal cost path for this timeframe is determined between the updated template locations. This procedure is repeated in pair-wise order until the centerlines in all time frames are obtained.

To illustrate the procedure, a post-processed image is shown in Fig. 2, together with the extracted coronary arteries at the end-diastolic phase for this data set. Starting point S_0 and ending point E_0 are selected from the right coronary artery in this image. Templates are then constructed at these two points to fit with the vessel segments in the same image. Points S_0 and E_0 are then transformed to next time frame in order to construct the initial templates. Then they are fitted to the local region of the image at corresponding time frame. For illustration, in Fig. 3, a random vessel position is chosen in one image. It shows the initial template position and its position after template fitting.

3. RESULTS AND EVALUATION

To assess the performance of the two motion tracking strategies we have performed experiments on five cardiac CT sequences. All of the CT image sequences have twenty phases with various image dimensions ranging from 256×256×89 to 256×256×188 voxels. Three datasets have voxel dimensions of 0.7×0.7×0.8 mm^3. The other two datasets have voxel dimensions of 0.64×0.64×1.5 mm^3. All datasets have various degrees of artifacts that affect the segmentation and registration procedure. In particular the fast motion of the heart in some time frames can lead to blurring or ghosting artifacts, e.g. around the coronary artery. As a result of this the non-rigid registration-based approach can only compensate for part of the deformation as shown Fig. 4.

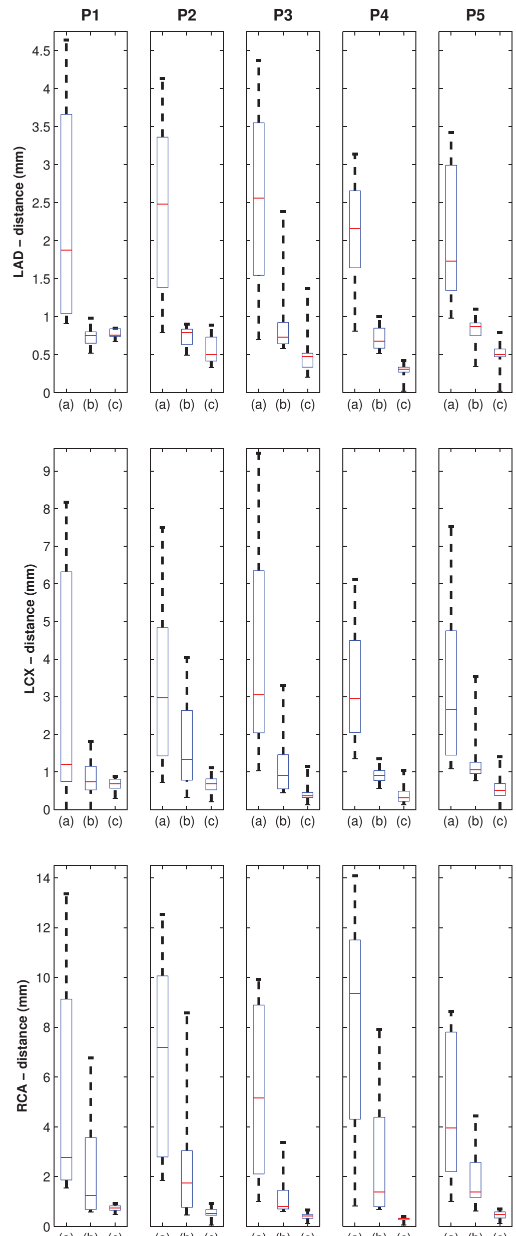

Fig. 4. The total coronary displacement (LAD, LCX, RCA) is shown in column (a). The residual coronary displacement after non-rigid registration is shown in column (b) and after template-based tracking is shown in column (c). The results show that the template-based tracking is able to model the coronary motion best.

In order to have a gold standard to evaluate the two different motion modeling approaches, the left anterior descending artery (LAD), left circumflex artery (LCX) and right coronary artery (RCA) are extracted using the minimal cost path algorithm from five CT sequences, P1, P2, P3, P4, and P5. In all five patients, the start and end points of the vessels have been identified manually and the results of the minimal cost path extraction has been judged as correct. The results of this are compared with the motion estimates of the LAD, LCX and RCA as provided by the non-rigid registration and template matching based approaches. To measure the agreement between the gold standard and the motion tracking approaches, a distance measure as proposed in [15] is used to quantify the coronary motion tracking errors. The results are shown in Fig. 4. The initial displacement of each coronary artery is computed as the distance between the centerline at end-diastole phase and the centerline at each other phase and is shown in the first column (a). The second column (b) shows the tracking error from non-rigid registration based approach. It is measured as the distance between centrelines estimated via non-rigid registration and the gold standard for each phase. The third column (c) shows the tracking error using the template matching approach. Again, it is measured as the distance between centrelines estimated via template fitting and the gold standard for each phase.

To measure whether the errors are significantly reduced using the template fitting method compared to the non-rigid registration method, a non-parametric Kruskal-Wallis test is performed to compare the errors obtained for each vessel and for each subject using these two methods. The results of this analysis is shown in Table 1 . We consider that the errors are significantly smaller using template-based approach when p-value of the test is below 0.05.

Table 1. P-values of Kruskal Wallis test on the errors

	P1	P2	P3	P4	P5
LAD	0.44	0.0093	1.7e-06	1.2e-07	0.0018
LCX	0.43	0.0015	1.2e-04	1.4e-06	1.7e-05
RCA	0.049	2.6e-05	2.1e-07	6.2e-07	1.8e-07

4. CONCLUSIONS AND FUTURE WORK

We have presented a novel approach for patient-specific coronary artery segmentation and motion modeling from cardiac CT sequences which combines the template matching and graph search algorithm. The proposed method has been tested on five clinical CT datasets. By constructing a 4D motion model of the coronaries from pre-operative cardiac images and aligning the 4D coronary model with the series of 2D endoscopic images acquired during the operation, we aim to assist the surgical planning and provide image guidance in robotic-assisted totally endoscopic coronary artery bypass (TECAB) surgery. Through this work, we expect to reduce the conversion rate from TECAB to conventional invasive procedures.

5. REFERENCES

[1] F. W. Mohr, V. Falk, A. Diegeler, T. Walther, J. F. Gummert, J. Bucerius, S. Jacobs, and R. Autschbach, "Computer-enhanced "robotic" cardiac surgery: Experience in 148 patients," *Journal of Thoracic and Cardiovascular Surgery*, vol. 121, no. 5, pp. 842 – 853, 2001.

[2] S. Dogan, T. Aybek, E. Andressen, C. Byhahn, S. Mierdl, K. Westphal, G. Matheis, A. Moritz, and G. Wimmer-Greinecker, "Totally endoscopic coronary artery bypass grafting on cardiopulmonary bypass with robotically enhanced telemanipulation: Report of forty-five cases," *Journals of Thoracic Cardiovascular Surgery*, vol. 123, pp. 1125–1131, 2002.

[3] M. Figl, D. Rueckert, D. Hawkes, R. Casula, M. Hu, O. Pedro, D. P. Zhang, G. Penney, F. Bello, and P. Edwards, "Augmented reality image guidance for minimally invasive coronary artery bypass," in *Proc. SPIE*, 2008, vol. 6918.

[4] M. Figl, D. Rueckert, D. Hawkes, R. Casula, M. X. Hu, O. Pedro, D. P. Zhang, G. Penney, F. Bello, and P. Edwards, "Coronary motion modelling for augmented reality guidance of endoscopic coronary artery bypass," in *ISBMS: Proceedings of the 4th international symposium on Biomedical Simulation*, 2008, pp. 197–202.

[5] G. Shechter, F. Devernay, A. Quyyumi, E. Coste-Maniere, and E. McVeigh, "Three-dimensional motion tracking of coronary arteries in biplane cineangiograms," *IEEE Transactions in Medical Imaging*, vol. 22(4), pp. 493–603, 2003.

[6] G. Shechter, J. R. Resar, and E. R. McVeigh, "Displacement and velocity of the coronary arteries: cardiac and respiratory motion," *IEEE Transactions on Medical Imaging*, vol. 25, pp. 369–375, 2006.

[7] C. Metz, M. Schaap, S. Klein, L. Neefjes, E. Capuano, C. Schultz, R. J. van Geuns, P. W. Serruys, T. van Walsum, and W. J. Niessen, "Patient specific 4D coronary models from ECG-gated CTA data for intra-operative dynamic alignment of CTA with X-ray images," *MICCAI (1)*, vol. 5761, pp. 369–376, 2009.

[8] A. C. Weustink, N. R. Mollet, F. Pugliese, W. B. Meijboom, K. Nieman, M. H. Heijenbrok-Kal, T. G. Flohr, L. A. Neefjes, F. Cademartiri, P. J. de Feyter, and G. P. Krestin, "Optimal electrocardiographic pulsing windows and heart rate: Effect on image quality and radiation exposure at dual-source coronary CT angiography," *Radiology*, vol. 248, no. 3, pp. 792–798, September 2008.

[9] K. Zuiderveld, "Contrast limited adaptive histogram equalization," in *Graphics gems IV*, pp. 474–485. Academic Press Professional, Inc., San Diego, CA, USA, 1994.

[10] J. Weickert, *Anisotropic Diffusion In Image Processing*, Teubner-Verlag, Stuttgart, Germany, 1998.

[11] A. Frangi, W. Niessen, R. Hoogeveen, T. van Walsum, and M. Viergever, "Model-based quantitation of 3D magnetic resonance angiographic images," *IEEE Transactions on Medical Imaging*, vol. 18, no. 10, pp. 946–956, 1999.

[12] P. E. Hart, N. J. Nilsson, and B. Raphael, "A formal basis for the heuristic determination of minimum cost paths," *IEEE Transactions on Systems Science and Cybernetics*, vol. 4, no. 2, pp. 100–107, 1968.

[13] D. Rueckert, L. I. Sonoda, C. Hayes, D. L. Hill, M. O. Leach, and D. J. Hawkes, "Nonrigid registration using free-form deformations: application to breast MR images.," *IEEE Transactions on Medical Imaging*, vol. 18, no. 8, pp. 712–721, 1999.

[14] O. Friman, M. Hindennach, and H. O. Peitgen, "Template-based multiple hypotheses tracking of small vessels," in *5th IEEE International Symposium on Biomedical Imaging: From Nano to Macro*, 2008, pp. 1047–1050.

[15] D. P. Zhang, E. Edwards, L. Mei, and D. Rueckert, "4D motion modeling of the coronary arteries from CT images for robotic assisted minimally invasive surgery," in *Proc. SPIE*, 2009, vol. 7259.